Available online at www.sciencedirect.com
ScienceDirect
Computer Physics Communications 177 (2007) 98–101
Computer Physics Communications
www.elsevier.com/locate/cpc

Development of a parallelized 3D electrostatic PIC-FEM code and its applications

J.-S. Wu *, K.-H. Hsu, F.-L. Li, C.-T. Hung, S.-Y. Jou

Mechanical Engineering Department, National ChioTung University, Hsinchu 30050, Taiwan

Available online 23 February 2007

Abstract

A parallelized three-dimensional self-consistent electrostatic particle-in-cell (PIC) code using unstructured tetrahedral mesh is proposed. Parallel implementation of the current unstructured PIC-FEM code is realized on distributed-memory PC-cluster system utilizing dynamic domain decomposition. Completed code is verified by simulating a quasi-1D RF argon gas discharge with results comparable to previous experimental observations and simulations. Parallel performance with dynamic domain decomposition of the PIC code is tested using a 3D RF argon gas discharge on a PC-cluster system. Results show that parallel efficiency can achieve 83% at 32 processors with dynamic domain decomposition. Some possible improvement of the code performance is demonstrated. Completed code is then applied to predict field emission without and with space-charge effect, and to simulate the RF magnetron argon plasma to demonstrate its capability in handling practical problems.

Keywords: Particle-in-cell; Finite element; Tetrahedral mesh; Parallel implementation; Dynamic domain decomposition

1. Introduction

Recently, PIC method using unstructured mesh has begun to appear in the literature, although there are very few. Two recent examples using unstructured tetrahedral mesh include Celik et al. [1] and Spirkin and Gatsonis [2]. In the former, they only tracked ions by assuming Boltzmann relation for electrons and applied Newton iterative algorithm for solving the nonlinear Poisson's equation which was discretized using finite element method (FEM). Although the simulation was efficient, assumption of Boltzmann relation for electrons may not be correct for most of the low-temperature plasma flows that are non-equilibrium in nature. In the latter, both ions and electrons are tracked at the same time, and the Poisson's equation, which was discretized using finite volume method (FVM), was solved using conjugate gradient method. In this study, only very small problem size was demonstrated because of several major reasons, including the inefficient equation solver, the slow particle tracking on unstructured mesh and being lack of parallel processing.

In addition, there are very few studies in parallel processing of PIC method using dynamic domain decomposition, which is important for particle-based method to achieve better load balancing. The only two examples in the literature to the authors' best knowledge are the studies by Seidel et al. [3] and Liewe and Decyk [4] using structured grids, in which the method dynamically repartitioned the computational domain that is intended to balance the workload among processors. In these studies, domain decompositions for particles and equation solver are different, which requires intensive communication at each time step.

Motivated by the above reviews, in the current study we intend to develop and verify a parallelized PIC-FEM code using 3D unstructured tetrahedral mesh with dynamic domain decomposition for applications that involve charged particles. In addition, several applications using the completed PIC-FEM code are demonstrated.

2. Parallel PIC-FEM using tetrahedral mesh

2.1. PIC-FEM on unstructured mesh

Proposed PIC-FEM on unstructured mesh is fundamentally very similar to the conventional PIC method on structured

* Corresponding author.
E-mail address: chongsin@faculty.nctu.edu.tw (J.-S. Wu).

0010-4655/$ – see front matter
doi:10.1016/j.cpc.2007.02.059

mesh. In short, the present explicit PIC-FEM method consists of the following steps: (1) Initialization; (2) Charge assignment to each grid points; (3) Calculation of electromagnetic field; (4) Force interpolation to each particle; (5) Pushing all particles; (6) Monte Carlo collision of particles; (7) Indexing all the particles; (8) Reducing number of particles if exceeding preset maximal number of particles; (9) Sampling the particles within cells to determine the macroscopic quantities; (10) Repeat steps 2–9 if maximum number of time steps is not reached. In the above the linear shape functions in FEM are used for charge assignment and field interpolation, in addition to the finite element simulation of Poisson's equation. In solving the Poisson's equation, we have utilized parallel conjugate gradient (CG) based on subdomain-by-subdomain method [7]. The reason to index all particles to where the cells the reside is to keep the flexibility of adding DSMC module for collisions of neutral species in the future.

2.2. Parallel implementation with dynamic domain decomposition

2.2.1. Parallel implementation

The proposed parallel code is implemented using MPI with SPMD paradigm on a distributed-memory machine, such as a PC-cluster system used in the present study. Communication is required at two instants for each time step. One is when particle moves across the inter-processor boundary (IPB), which requires the communication of particle data (coordinates, velocities, charge). These data are sent to the destination processor by pre-packing together into a buffer array and are sent as a whole during communication. The other is when Poisson's equation is solved, which requires the communication of field data (potential, electric field, magnetic field) across the IPB. The same domain decomposition is used for both the particle and field solvers in the current study. This can reduce the possible communication load as proposed in Liewe and Decyk [4], which divided the spatial domain into primary (particle) and secondary (field equation) decompositions that are different in general.

2.2.2. Dynamic domain decomposition

In the current study, a dynamic domain decomposition (DDD) module similar to that in Wu and Tseng [5] is developed to relieve this concern of load unbalancing. Important features of this DDD include decision mechanism of when to repartition, repartitioning the domain using a multi-level graph-partitioning tool and reordering the data structure in each processor according to the new partition. Details can be found in [5] and are skipped for brevity.

3. Results and discussion

3.1. Verifications

3.1.1. Quasi-1D RF gas discharge

A quasi-1D argon gas discharge with application of a RF (13.56 MHz) voltage source at the cathode and grounded anode [6] is considered to verify the parallel PIC-MCC code. Results have shown that nearly single Maxwellian and bi-Maxwellian EEPF for high (50 mTorr) and low (20 mTorr) is demonstrated using this PIC-FEM code, respectively.

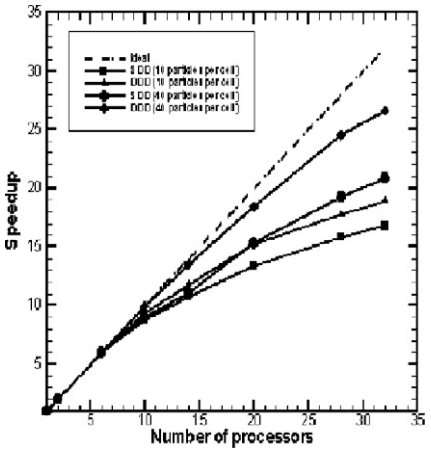

Fig. 1. Parallel speedup as a function of the number of processors (HP-Itanium 64-bit, dual processors per node).

3.2. Code performance study

3.2.1. Performance of PIC-FEM code

To test the parallel performance of the current parallel PIC-MCC code using dynamic domain decomposition, we have simulated the plasma within a 3D RF gas discharge chamber. Considering geometrical symmetry, we only use 1/16 of the full chamber for simulation with ∼0.16 million tetrahedral cells. Speedup test is conducted on HP-IA (64-bit) clusters parallel machines (distributed-memory) up to 32 processors.

Fig. 1 illustrates the resulting speedup as a function of the number of processors. Results show that speedup increases with increasing number of simulation particles per cell. As number of particles increases, most of the computational load goes to the particle-related simulation, which has better speedup in general using domain decomposition method as compared to the equation solver. For number of particles per cell increases over 40, the speedup should be better since the computational load shared by the equation solver becomes even less. Using 32 processors, parallel efficiency as high as 83% can be obtained if ∼40 particles/cell is used, while only 58% can be obtained if ∼10 particles/cell is used. Reason of good parallel efficiency using DDD can be clearly seen from Fig. 2 which shows the evolution of the domain decomposition during runtime.

3.3. Possible improvements

There are two possible improvement we could made regarding the PIC-FEM code, including the particle tracing on unstructured mesh and the Poisson's equation solver. In the former, we have proposed a so-called Almost Trackless Algorithm (ATA) to efficiently track the particles on an unstructured mesh by taking advantage of necessity of charge-to-node assignment for each particle and very small time step constrained

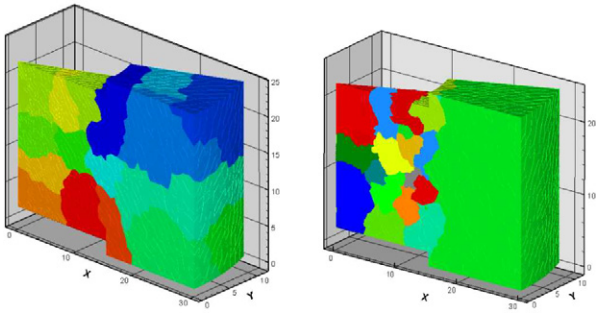

Fig. 2. Evolution of domain decomposition. Initial (left); final (right).

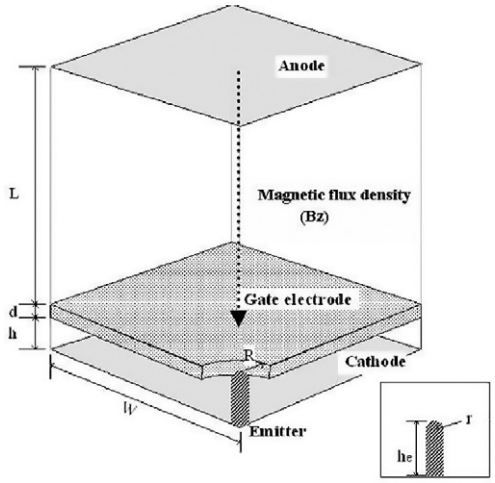

Fig. 3. Schematic diagram of the 1/4 simulation domain for a typical CNT-based triode-type field emitter within a periodic cell. Important geometrical parameters are: $R = 500$ nm, $r = 10$ nm, $he = 600$ nm, $h = 500$ nm, $d = 200$ nm, $L = 0.9$ mm and $W = 0.3$ mm.

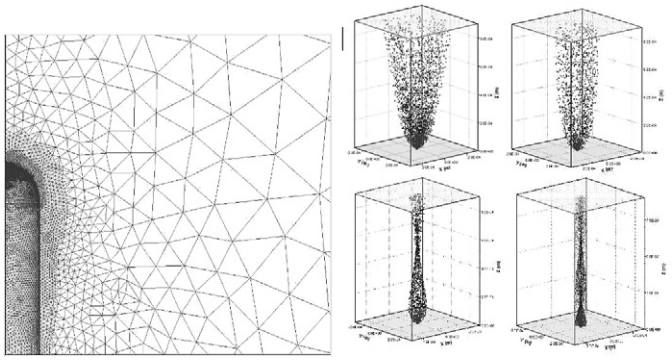

Fig. 4. From left to right, top to bottom: Exploded view of the refined mesh near the tip, instantaneous snapshot of electrons from a single-CNT triode-type field emitter with $B = 0, -0.2, -0.5, -1.0$ Tesla. The gate voltage and the anode voltage are fixed at 120 Volts and 1 kV, respectively.

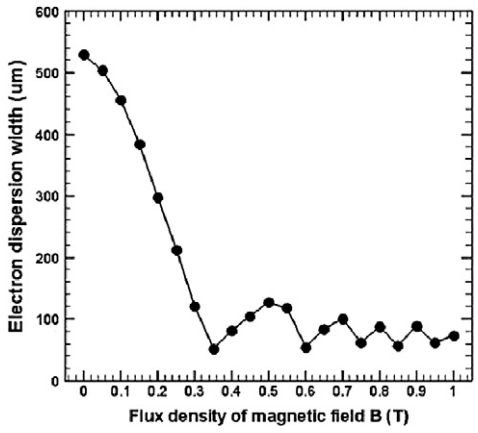

Fig. 5. Dependence of electron beam diameter at the anode on the flux density of magnetic focusing field.

by $\Omega_e \sim 0.2$. Preliminary results show that the particle-tracing time can be reduced ~5 times. In the latter, we have implemented an one-level and zero-level (or block-Jacobi) overlapping additive Schwarz method (ASM) [7] for the discretized Poisson's equation. Preliminary tests for a problem of ~51,000 nodes using 32 processors show that the speedup is about 1.5 and 2.0 for one-level and zero-level ASM preconditioning, respectively, as compared to the pure CG. Indeed, more tests of the above two possible improvements are needed in the very near future. However, the above two improvements are not employed for the following applications.

3.4. Applications

3.4.1. Field emission prediction

Without space-charged effect. We simulate the field emission from a gated single-CNT triode-type field emitter with an applied uniform downward magnetic field, as shown in Fig. 2. Note this downward magnetic field can be achieved in practice using either coils or permanent magnets around the emission cells [8]. By assuming the electric field and magnetic field do not change due to the emitted electrons, the Poisson's equation is solved only once through the use of a PAMR (parallel adaptive mesh refinement) module [9], which can automatically refine the mesh near the tip of the single CNT (top-left of Fig. 3), where the electric field is very large. Simulation, considering the Fowler–Nordiem emission law [10] at the cathode surface, shows that electron beam diameter at the anode decreases with increasing applied downward magnetic field (Fig. 4), while the value oscillating around 70 nm with decreasing amplitude as the **B** is greater than ~0.35 Tesla, which is shown in Fig. 5, mainly because of the over focusing induced by large **B**.

With space-charged effect. In addition, we simulate field emission from a emitter made of nano-silicon tip (diameter ~90 nm) under vacuum due to a tungsten anode with the gap distance of ~60 nm. In this simulation, the PAMR module is also applied to refine the mesh near the nano-tip by using the initial potential distribution without considering the space-charge effect. Considering the F-N emission law at the cathode surface, the PIC-FEM code is then run to simulate the field emission self-consistently very 10 time steps by turning off the MC module. As shown in Fig. 6, the predicted I–V curve with work function of 4.5 eV compares surprisingly well to the measurements. In addition, the predicted turn-on voltage is 175 V which is within 5% of the experimental value. Note simulated field emission current is at least 30 times larger as the correct

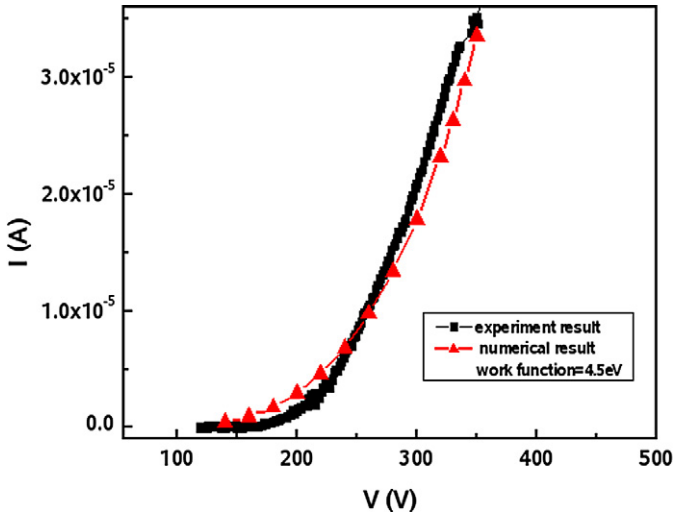

Fig. 6. Comparison of simulated and measured I–V curve.

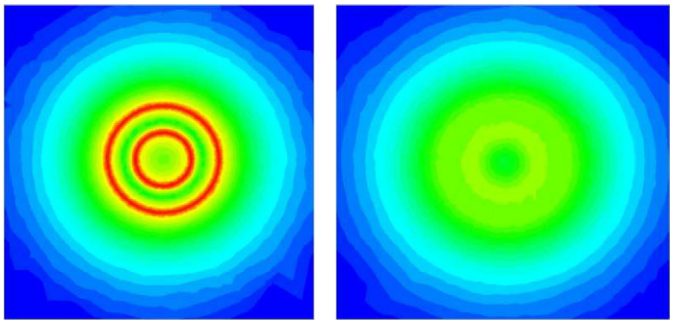

Fig. 7. Magnetic field strength at the mid-cross section of PM (left) and 0.002 m above the target electrode.

one if space charges due to the emitted electrons were not considered in the simulation.

3.4.2. RF magnetron plasma simulation

Finally, we simulate a 3D RF magnetron plasma within a chamber with circular permanent magnets underneath the cathode. The distribution of magnetic field inside the chamber is simulated by solving the vector magnetic potential equation using FEM as shown in Fig. 7 with magnetization strength $M = 0.35$ Tesla of the two concentric permanent magnets. Simulation conditions include: argon gas, gas pressure $P = 5$ mTorr, gas temperature $T = 300$ K, diameter of both electrodes $d = 120$ mm, distance between electrodes $L = 50$ mm, applied RF frequency $f_{RF} = 13.56$ MHz, applied RF voltage $V_{p-p} = 600$ Volts, secondary electron emission $\gamma = 0.06$ at the cathode, ~0.3 mills ion cells, ~7.5 million particles (at quasi-steady state) and $\Delta t_e = 3.76\text{E}{-}11$ seconds. Parallel processing with DDD and 28 processors is applied. Type of collisions include elastic collisions between Ar–Ar and excitation of Ar, ionization of Ar by electron and elastic collisions between Ar^+–Ar. Data are sampled after 300 RF cycles. Fig. 8 shows the cycle-averaged number density distributions of electrons and ions, while others are skipped due to the limit of the paper length.

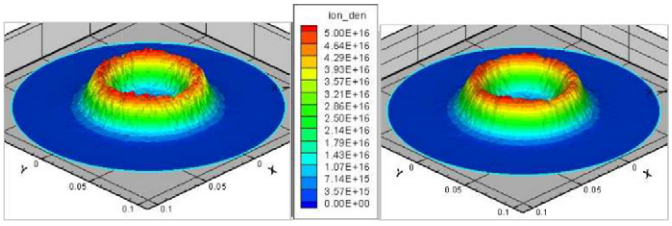

Fig. 8. Cycle-averaged distributions of number densities of electrons (left) and ions (right) for a RF magnetron argon plasma.

4. Summary

In the present study, we have developed a parallelized electrostatic PIC-FEM code using unstructured tetrahedral mesh, which is portable among distributed-memory parallel machines. Completed code is then applied to predict field-emission properties and to simulate a RF magnetron plasma to demonstrate its wide applicability in various disciplines of research.

Future direction of researches includes adding the DSMC simulation capability into the present PIC-FEM code, adding a previously developed Maxwell's equation solver using edge-based FEM and applying the PIC-FEM to study more interesting and important problems.

Acknowledgements

This work was supported in part by the National Science Council of Taiwan, with grants NSC-932212-E-009-015 and NSC 93-2212-E-009-015.

References

[1] M. Celik, M. Santi, S. Cheng, M. Martinez-Sanchez, J. Peraire, in: 28th Internat. Electric Propulsion Conference, Toulouse France, 2003, IEPC-03-134.
[2] A. Spirkin, N.A. Gatsonis, Comput. Phys. Comm. 164 (2004) 383.
[3] D.B. Seidel, S.J. Plimpton, M.F. Pasik, R.S. Coats, G.R. Montry, Pulsed Power Plasma Sci. 2 (2002) 1000.
[4] P.C. Liewe, V.K. Decyk, J. Comp. Phys. 85 (1989) 302.
[5] J.-S. Wu, K.C. Tseng, Int. J. Num. Meth. Eng. 63 (2005) 37.
[6] V.V. Serikov, S.S. Kawamoto, K. Nanbu, IEEE Trans. Plasma Sci. 27 (1999) 1389.
[7] Y. Saad, Iterative Methods for Sparse Linear Systems, first ed., Society for Industrial and Applied Mathematics, Philadelphia, 2003.
[8] N. Egami, M. Nanba, Y. Takiguchi, K. Miyakawa, T. Watabe, S. Okazaki, K. Osada, Y. Obara, M. Tanaka, S. Itoh, J. Vac. Sci. Technol. B 23 (2005) 2956.
[9] Y.-Y. Lian, K.-H. Hsu, Y.-L. Shao, J.-S. Wu, Comput. Phys. Comm. (2006).
[10] R.H. Fowler, L. Nordheim, Proc. Roy. Soc. A (London) 119 (1928) 173.